IEEE Access
Multidisciplinary ⋮ Rapid Review ⋮ Open Access Journal

Received March 29, 2020, accepted April 15, 2020, date of publication April 21, 2020, date of current version May 7, 2020.

Digital Object Identifier 10.1109/ACCESS.2020.2989199

MMQT: Maximizing the Monitoring Quality for Targets Based on Probabilistic Sensing Model in Rechargeable Wireless Sensor Networks

WEN-HWA LIAO[1,2], (Member, IEEE), BHARGAVI DANDE[3], CHIH-YUNG CHANG[3], (Member, IEEE), AND DIPTENDU SINHA ROY[4]

[1]School of Economics and Management, Chuzhou University, Chuzhou 239000, China
[2]Department of Information Management, Tatung University, Taipei city 10452, Taiwan
[3]Department of Computer Science and Information Engineering, Tamkang University, New Taipei City 25137, Taiwan
[4]Department of Computer Science and Engineering, National Institute of Technology Meghalaya, Shillong 793003, India

Corresponding author: Chih-Yung Chang (cychang@mail.tku.edu.tw)

This work was supported in part by the Key project of Humanities and Social Sciences in Anhui Universities under Grant SK2018A0429.

ABSTRACT In wireless sensor networks (WSNs), target coverage is an important issue which aims at finding a set of sensors to monitor the targets for maximizing both the surveillance quality and network lifetime. However, most of them assumed that each sensor is battery powered and the Boolean Sensing Model (BSM) is applied. Sensors powered by battery have a limited lifetime while the BSM is difficult to reflect the physical features of sensing. This paper proposes target coverage mechanisms, called *C-MMQT* and *D-MMQT*, which consider the solar-powered sensors and allows the battery to be recharged for maintaining the perpetual lifetime of sensor networks. The proposed mechanisms apply the Probabilistic Sensing Model (PSM) and consider that different targets have different importance. Two challenges have been overcome in this paper. First, each sensor is well scheduled for switching between recharging and working states for maintaining its perpetual lifetime since its battery is solar powered. Second, the sensors that are able to monitor the common target are well scheduled for cooperative sensing to maximize the surveillance quality since PSM is applied. Two efficient sensor schedules are proposed to maximize the surveillance quality of the bottleneck target which has the lowest surveillance quality. Performance study shows that the proposed mechanisms outperform the existing mechanisms in terms of Quality of Monitoring, Average utility, Fairness and Efficiency index.

INDEX TERMS Energy harvesting, scheduling, solar power, target coverage, wireless sensor networks.

I. INTRODUCTION

Wireless sensor networks (WSNs) are composed of many sensor nodes that are randomly deployed in the monitoring area. These sensors are tiny devices that are embedded with microcontroller unit, sensing and communication hardware components for supporting functions including data processing, communication and sensing [1], [2].

In general, sensor devices have some resource limitations, including battery life cycle, computational power and memory. Therefore, during the network operation, the energy efficiency of nodes plays a major role because the replacement of the battery is not possible in most of the applications [3]. According to different applications, coverage problems are classified into three categories. The first one is barrier coverage which aims to schedule a minimal number of sensors to detect the intruder crossing a boundary region. The second one is area coverage, which aims to schedule a set of sensors to monitor a given area such that the number of working sensors is minimal while the monitoring region contains no coverage hole. The last one is target coverage, which aims to monitor a given set of targets with the highest surveillance quality. In WSNs, the target coverage problem is one of the most important issues where sensors are responsible for monitoring the important targets and reporting if any suspicious event occurs near these targets.

Since sensors are generally powered with batteries that have limited energy, efficiently scheduling the sensors is an important concern for better energy management of a given WSN. Recent studies are divided into two categories for

The associate editor coordinating the review of this manuscript and approving it for publication was Nabil Benamar.

prolonging the network lifetime, the first category is energy conservation technologies [1]–[5] while the second category is energy transfer technologies [6]–[15].

Energy conservation techniques have been widely discussed in WSNs. In the past years, studies [1]–[5] proposed several sleep-awake scheduling mechanisms for energy conservation of the sensor nodes. By applying the scheduling mechanisms, sensors can periodically switch between sleep and awake modes. The sensor saves its energy consumption in the sleep mode while it performs the sensing and communication tasks in the awake mode. However, reducing the energy expenditure rate can only prolong the network lifetime. The sensors eventually exhaust their energy even when they apply the efficient sleep-awake mechanisms.

To achieve the perpetual lifetime of sensor networks, recent studies [6]–[15] proposed battery charging technologies. In literature, these studies can be further classified into two categories: wireless energy transferring and environmental energy harvesting technologies.

The wireless energy transferring technologies [6]–[10] mainly transmitted the electrical energy from a power transmitter to a power receiver without the interconnecting wires. The wireless power transmitter periodically moved towards the sensor and then recharge its battery when the sensor runs out of its battery. Studies [6]–[10] assumed that wireless power transmitters were mobile sinks and they can recharge the sensor to support its perpetual lifetime. However, the wireless power transmitter took a long time and consumed a large amount of energy to visit all the sensor nodes, especially for a large-scale monitoring region. On the other hand, environmental energy harvesting [11]–[15] is an efficient way to cope with the energy problem. There are lots of environmental energy resources, such as wind, solar, thermal and so on. Solar power is the most promising among all of the environmental energy resources [16]. Using solar power, the sensors can recharge its battery without mobile sink moving toward any sensor because the scale of sunlight is extensive. As a result, environmental energy harvesting can reduce the extra energy consumption.

To avoid the hardware cost for the replacement of battery and the energy consumption of wireless power transmitters, this paper investigates the target coverage issue for the solar-powered sensor networks. The challenge is that energy harvesting is usually insufficient to support the uninterrupted operations of sensors. In general, it is necessary to make a duty cycle for scheduling each sensor staying in charging or working states. It is a fact that the surveillance quality of each target for a given time slot highly depends on the cooperative sensing of those sensors staying in the working state in a certain time slot. Consequently, how to schedule the sensors such that the lowest surveillance quality can be maximized is still a big challenge and needs to be further investigated.

This paper assumes that the sensor nodes can recharge its battery while monitoring the point of interests (*POI*s) at the same time, which reflects the capability of the most practical sensors. The event detection probability for each *POI* depends on the distance between the sensor and the *POI*. The problem is how to design an activation schedule for the sensors to achieve the highest surveillance quality while maintaining the perpetual operation of the networks.

The key contributions of the proposed *MMQT* mechanisms are itemized as follows:

A. MAINTAINING THE PERPETUAL NETWORK LIFETIME

The proposed *MMQT* mechanisms consider the working and recharging schedules for maintaining their perpetual lifetime. This strategy further guarantees that the recharged energy of each sensor satisfies the required energy for working operations in each cycle.

B. CONSIDERING THAT POIs HAVE DIFFERENT IMPORTANCE

Different from existing studies [11]–[15], the proposed algorithm considered that different *POI*s might have different importance since they play different roles depending on the tasks. The proposed *MMQT* guarantees that the *POI*s with the higher importance would have a higher quality of monitoring (*QoM*).

C. THE PHYSICAL FEATURES OF THE SENSOR ARE TAKEN INTO CONSIDERATION

This paper applies the PSM to evaluate the surveillance quality which can reflect the physical features of sensing. Most of the existing works [12]–[15] applied BSM to develop the target coverage algorithms. Their estimations of coverage quality were not accurate and might result in coverage holes in the applications.

D. ACHIEVING HIGH SURVEILLANCE QUALITY FOR EACH POI

Study [14], [15] did not guarantee that all the *POIs* in the sensor network are covered at any given time. The proposed *MMQT* achieves high surveillance quality for each *POI* by allocating an unscheduled sensor to cooperatively monitor the bottleneck *POI* which has the lowest surveillance quality. As a result, the surveillance quality of the bottleneck *POI* can be improved and hence the minimal surveillance quality of the *POIs* is likely to be maximized.

The rest of the paper is organized as follows. Section II reviews the related work and compares them with the proposed *MMQT*. Section III presents the assumptions, network model and problem formulation. Section IV gives detailed descriptions of the activation scheduling algorithms. Section V investigates the performance improvements against the existing studies. Finally, section VI gives the conclusion and future work of this study.

II. RELATED WORK

This section presents the existing studies related to the target coverage issue in WSNs. In literature, these studies can be divided into two categories: energy conservation and the solar-powered categories.

TABLE 1. Comparisons of the proposed *MMQT* and existing mechanisms.

Studies	*POIs* have different importance	Guarantee target coverage	Balancing the *QoM* of *POIs*	Probabilistic sensing model	Can recharge and monitor at the same time
[11]	×	N/A	×	×	×
[12]	×	×	×	×	×
[13]	×	×	×	×	×
[14]	×	×	×	×	×
[15]	×	×	×	×	○
The proposed *MMQT*	○	○	○	○	○

Related studies fall in the energy conservation category assumed that each sensor is battery powered. To extend the network lifetime, most of them scheduled the sensor nodes staying in sleep and the awake modes in turn. In studies [1]–[3], the sensors decided their activation schedule in a distributed manner according to the neighboring information. The sensors were partitioned into a number of subsets, and each of them would take turns to cover the *POI*s. Although the proposed approaches can prolong the network lifetime, the energy balance issue between different subsets of sensors did not be considered. Study [4] proposed an activation scheduling approach which further considered the density and the energy consumption of each subset of the sensors. Study [5] considered the communication of all sensors and proposed a topology control protocol which can separate the sensors into specific subsets, and maintain the communication of the network. Although studies [1]–[5] can increase the network lifetime of sensors, they did not consider that the sensors can recharge its battery by the environmental energy harvesting. As a result, the battery of the sensor will drain as time goes by.

To provide the perpetual operation of wireless sensor networks, some other studies [11]–[15] fall in the solar-powered category which assumed that the battery of each sensor can be recharged by solar power. Study [11] proposed a robust target coverage for energy harvesting wireless sensor networks. This study considered three novel robust coverage requirements. First, sensor nodes must not expend more than their total harvested energy over T time slots. Second, the energy expenditure of each sensor node should not exceed the energy harvested in each slot. Finally, the energy expenditure of sensor nodes should not exceed the energy accumulated in the current slot. Furthermore, they considered the random energy arrivals in the network and ensures all the targets are monitored continuously. However, it could not guarantee that all the *POI*s are covered at any given time.

Study [12] addressed the target coverage problem in a solar-powered sensor network where each sensor can control its sensing range. Study [13] investigated the target coverage problem and aimed at maximizing the network lifetime of rechargeable wireless sensor networks. It scheduled sensors in a way that one subset of sensors stayed in an active state while other sensors stayed in a sleep state to recharge their battery. It proposed a linear programming based solution to determine the activation schedule of sensor nodes. Although studies [12] and [13] considered the solar-powered sensors and provides the perpetual operation of wireless sensor networks, they did not consider that different *POI*s have different importance.

Study [14] considered the quality-aware target coverage problem in an energy harvesting sensor network. For a given monitoring period, the sensors were powered by renewable energy sources and operated in a duty cycle mode. It scheduled a different subset of sensors to be activated in each time slot. As a result, the coverage quality was increased with the number of time slots in which a target was covered. Although study [14] aimed to maximize the coverage quality of the entire network, they did not consider how to balance the *QoM* of each *POI*s at any given time and cooperative sensing among sensors.

Study [15] proposed a greedy hill climbing activation scheme which assumed that sensors can either recharge its battery or monitor *POI*s at the same time. The detection probability of a sensor to some *POI* depends on the distance between the sensor and *POI*. The proposed approach firstly calculated the ratio between the recharge and discharge time as its charging period to ensure a sensor can supply the energy which was consumed in the working period. Then it scheduled a sensor to be active in a time-slot aiming to maximize the incremental utility together with the sensor previously scheduled. Although it provided the perpetual operation of wireless sensor networks and maximize the *QoM* of the entire network, it cannot guarantee that all the *POI*s are covered at any given time. Furthermore, it did not consider the different importance of different POIs.

The studies [11]–[15] considered the schedule of sensors and the efficiency of solar power. However, they did not consider how to balance the *QoM* of each *POI*s at any given time. Furthermore, they did not consider the issue that *POI*s might have different importance. Table 1 summaries the comparisons between this paper and the existing studies which considered the solar-powered sensor networks. This paper investigates the target coverage problem by considering the PSM. The objective of this paper is to maximize the *QoM*

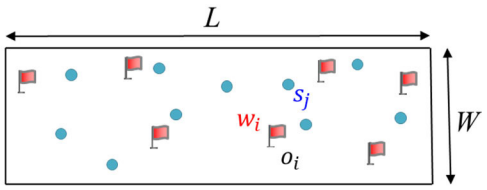

FIGURE 1. An example of the considered network.

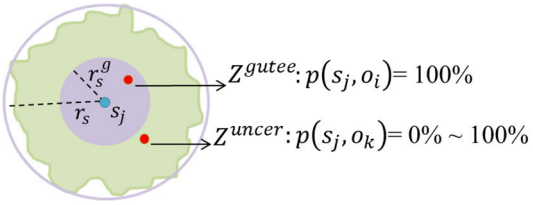

FIGURE 2. The applied Probabilistic Sensing Model.

of the target with minimal *QoM*. The cooperative sensing is taken into account. The proposed approaches schedule the sensors based on the two-dimensional space time points which consist of different targets and the time slots of each cycle. The cooperative sensing contribution of each sensor will be calculated for each space time point. In each run, one sensor that has the largest cooperative sensing contribution to the bottleneck space time point will be scheduled to be active at that point, aiming to maximize the *QoM* of the target with the minimal *QoM*. As a result, the weakest *QoM* among all targets will be maximized run by run while the perpetual network lifetime can be maintained.

III. NETWORK ENVIRONMENT AND PROBLEM FORMULATION

This section firstly introduces the network environment and assumptions of the considered solar-powered sensor networks. Then, the problem formulation of this study is presented.

A. NETWORK ENVIRONMENT

This paper assumes that a set of m *POI*s $O = \{o_1, o_2, \ldots, o_m\}$ is distributed over a two-dimensional region R with size L x W, where L and W are the length and width of R, respectively. Assume that *POI*s have different importance since they play different roles depending on the executing tasks. Let w_i be the weight of *POI* o_i. The *POI* with higher importance would have a larger weight value. In region R, there are a set of n solar-powered homogeneous sensors, denoted by $S = \{s_1, s_2, \ldots, s_n\}$, which are randomly deployed over the monitoring region. The sensing radius of each sensor is denoted by r_s, which is the same for all the sensors and the clocks of all sensors have been synchronized. Fig. 1 gives a scenario of the considered network where the flag and node represent the *POI* and sensor, respectively.

B. SENSING MODEL

In this paper, the Probabilistic Sensing Model (PSM) [17] is applied. The following gives an example to illustrate the PSM. As shown in Fig. 2, the red point denotes the *POI* which is monitored by the sensor s_j. The sensing range of any sensor s_j is divided into two regions, including the guarantee zone which is marked with a light violet color and the uncertain zone which is marked with light green color. Let Z^{gutee} and Z^{uncer} denote the guarantee and uncertain regions of the sensing range of any sensor, respectively. Let r_s^g and r_s denote the radiuses of Z^{gutee} and Z^{uncer}, respectively. When the event occurs in the region Z^{gutee}, the detection probability of sensor s_j is 100%. However, in case the event is occurred in Z^{uncer}, the detection probability of an event by the sensor s_j is decreased with the distance between the sensor s_j and *POI*.

Let $p\left(s_j, o_i\right)$ denote the detection probability of *POI* o_i by sensor s_j. Let $d\left(s_j, o_i\right)$ represents the Euclidean distance of the sensor s_j and the *POI* o_i. Exp. (1) presents the detection probability $p\left(s_j, o_i\right)$ of sensor s_j to *POI* o_i.

$$p(s_j, o_i) = \begin{cases} 1, & if\ d(s_j, o_i) \le r_s^g \\ e^{-\lambda(d\left(s_j, o_i\right) - r_s^g)^\gamma}, & if\ r_s^g < d\left(s_j, o_i\right) < r_s \\ 0, & if\ r_s \ge d\left(s_j, o_i\right) \end{cases} \quad (1)$$

where the parameters λ and γ are the path-loss exponents of the sensing signal strength and could be adjusted according to the physical properties of the sensor. Assume that the coordinates of s_j and o_i are $\left(x_j^s, y_j^s\right)$ and $\left(x_i^o, y_i^o\right)$, respectively. The distance $d\left(s_j, o_i\right)$ in Exp. (1) can be calculated by

$$d\left(s_j, o_i\right) = \sqrt{\left(x_j^s - x_i^o\right)^2 + \left(y_j^s - y_i^o\right)^2}.$$

C. RECHARGING AND DISCHARGING MODEL

Assume that each solar-powered sensor is energy constraint and rechargeable. Each sensor has four possible states, including *sensing-only*, *recharging-only, sensing & recharging* and *sleeping states*. Each sensor consumes energy when it stays in *sensing-only* state or *sensing & recharging* state. A sensor staying in *recharging-only* state can be recharged from the solar energy resource. In the *sensing & recharging* state, each sensor can perform the sensing and recharging operations simultaneously while the sensor staying in the *sensing-only* state will turn on its sensing component aiming to monitor the covered *POI*s. In the *sleeping* state, the sensors will not participate in sensing and other operations until it changes state. Since sensors can't be recharged at night, the sensor staying in *sensing-only* state can perform sensing operation.

In the *recharging-only* state, each sensor has to consume some energy to activate its solar-panel. Let e^{min} be the energy reserved for solar-panel activation. Let e^{rec} denote the energy that the sensor can obtain from the solar-power in the *recharging-only* state in one time slot. That is to say, in the *recharging-only* state, the sensors would gain $e^{rec} - e^{min}$ energy in one time slot. The sensors would collect some

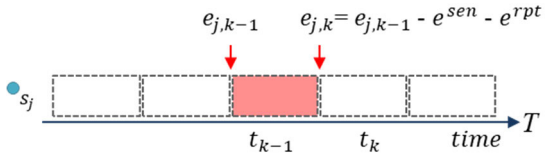

FIGURE 3. The residual energy of the sensor.

information from the *POI*s which they covered in the *sensing-only* state and transmit the information to the sink node after the *sensing-only* state. Therefore, they have to reserve certain energy for transmission after the *sensing-only* state. Let e^{sen} denote the energy consumption of sensors in one time slot in the *sensing-only* state, and e^{rpt} denote the reserve energy for the transmission after the *sensing-only* state. Therefore, the entire energy consumption of the sensors in the *sensing-only* state in one time slot is $e^{sen} + e^{rpt}$ and reserve at least e^{min} for triggering the recharge circuit. The energy of sensors does not change in the *sleeping* state.

This work used a simple battery model with no energy loss or leakage. Although the sensor can recharge its battery by solar power, we assume that the battery capacity is limited. As a result, the sensors cannot unlimitedly store the energy in the battery capacity. Let e^{max} be the upper bound of the battery capacity. Once the sensors remaining energy is less than e^{min}, then the sensor is treated as dead.

Fig. 3 depicts an example of residual energy of sensor s_j at different time slots. It is assumed that the recharge and discharge ratio is 4:1. Therefore, each sensor can stay in a sensing & recharging state for one time slot and stay in recharging-only state for the remaining four slots. Let $e_{j,k}$ denote the remaining energy of sensor s_j at the starting time point of the slot t_k. As shown in Fig. 3, if the sensor s_j was in the recharging-only state at time slot t_{k-1}, the $e_{j,k}$ is the smaller one between $e_{j,k-1}$ plus the increased energy e^{rec} and the upper bound of battery capacity e^{max}. If the sensor s_j was in the sensing-only state at time slot t_{k-1}, then $e_{j,k}$ is $e_{j,k-1}$ minus the energy consumption $e^{rpt} + e^{sen}$ at time slot t_{k-1}. The values of $\alpha_{j,k}^{rec}$, $\alpha_{j,k}^{sen}$ and $\alpha_{j,k}^{slp}$ are defined in Exps. (5), (6) and (7). Therefore, the residual energy of the sensor s_j at time slot t_k is given in the Exp. (2).

$$e_{j,k} = \begin{cases} \min\left(e_{j,k-1} + e^{rec}, e^{max}\right), & if\ \alpha_{j,k-1}^{rec} = 1 \\ e_{j,k-1} - \left(e^{sen} + e^{rpt}\right), & if\ \alpha_{j,k-1}^{sen} = 1 \\ e_{j,k-1}, & if\ \alpha_{j,k-1}^{slp} = 1 \end{cases}. \quad (2)$$

Let τ denote the length of a time slot. There are three physical parameters which impact the energy of each sensor, including battery capacity, discharging rate and recharging rate denoted by e^{max}, u^{sen} and u^{rec}. The values of e^{rec} and e^{sen} can be calculated by applying Exp. (3).

$$e^{rec} = \frac{e^{max} - e^{min}}{u^{rec}} \text{ and } e^{sen} = \frac{e^{max} - e^{min}}{u^{sen}} \quad (3)$$

Let κ denote the ratio of the discharging and recharging rates. The value of κ is shown in Exp. (4).

$$\kappa = \left\lceil \frac{e^{rec}}{e^{sen}} \right\rceil \quad (4)$$

The time line can be divided into several cycles, each cycle is denoted by T, which consists of ϑ equal sized time slots where $\vartheta = \kappa + 1$. It is obvious that the value of e^{rec} is κe^{sen} such that each sensor can recharge energy for consuming in the sensing state because each sensor has an identical schedule in each cycle.

Let t_k denote the k-th time slot in a cycle T. The following further defines three Boolean variables $\alpha_{j,k}^{rec}$, $\alpha_{j,k}^{sen}$ and $\alpha_{j,k}^{slp}$, which represent the operation of sensor s_j stays at time slot t_k. That is,

$$\alpha_{j,k}^{rec} = \begin{cases} 1, & \text{if } s_j \text{ performs recharging operation in } t_k \\ 0, & \text{otherwise.} \end{cases} \quad (5)$$

$$\alpha_{j,k}^{sen} = \begin{cases} 1, & \text{if } s_j \text{ perfroms sensing operation in } t_k \\ 0, & \text{otherwise.} \end{cases} \quad (6)$$

$$\alpha_{j,k}^{slp} = \begin{cases} 1, & \text{if } s_j \text{ sleeps in } t_k \\ 0, & \text{otherwise.} \end{cases} \quad (7)$$

For example, if the sensor s_j stays in sensing & recharging state at certain time slot t_k, then we have $\alpha_{j,k}^{rec} = 1$, $\alpha_{j,k}^{sen} = 1$ and $\alpha_{j,k}^{slp} = 0$.

D. PROBLEM FORMULATION

This paper addresses the target coverage problem for solar-powered sensor networks. Our objective is to propose an activation schedule algorithm for the sensors which aims to maximize the monitoring quality of the *POI* with the minimal quality of monitoring among all *POIs* under the constraint of perpetual network lifetime. This section initially introduces the objective function and then the constraints which should be satisfied when achieving the maximal value of the objective function.

Utility function: Let S_i denote the set of sensors that are able to monitor target o_i. That is,

$$S_i = \left\{s_j | d\left(o_i, s_j\right) < r_s\right\} \quad (8)$$

Let $S_{i,k}$ denote the set of the activated sensors that can monitor the *POI* o_i at time slot t_k. The value of $S_{i,k}$ can be evaluated as shown in Exp. (9).

$$S_{i,k} = \left\{s_j | d\left(o_i, s_j\right) < r_s \wedge \alpha_{j,k}^{sen} = 1\right\} \quad (9)$$

The following introduces the cooperative sensing probability among sensors which monitor the common object at the same time slot. The un detection probability of sensor s_j to target o_i is $1 - p\left(s_j, o_i\right)$. It implies that the probability of all sensors $s_j \in S_{i,k}$ not detecting the event occurred at the target o_i is

$$\prod\nolimits_{s_j \in S_{i,k}} \left(1 - p\left(s_j, o_i\right)\right).$$

Let $p_{i,k}$ denote the detection probability of *POI* o_i for any sensor $s_j \in S_{i,k}$ at time slot t_k. The value of $p_{i,k}$ can be derived by Exp. (10).

$$p_{i,k} = 1 - \prod_{s_j \in S_{i,k}} \left(1 - p\left(s_j, o_i\right)\right). \tag{10}$$

Let $u_{i,k}$ denote the detection probability of *POI* o_i at time slot t_k. This paper defines $u_{i,k}$ as the event detection probability $p_{i,k}$ divided by the weight of the *POI* o_i. That is,

$$u_{i,k} = \frac{1 - \prod_{s_j \in S_{i,k}} (1 - p(s_j, o_i))}{w_i}, \forall \alpha_{j,k}^{sen} = 1 \tag{11}$$

Definition: Quality of Monitoring (QoM)

Let u_i represent the *QoM* of *POI* o_i. As shown in Exp. (12), the u_i is defined as the minimum *QoM* of *POI* o_i in all possible time slots.

$$u_i = min(u_{i,k}) \forall t_k \tag{12}$$

The following presents the objective function and the constraints of the solar-powered sensor networks.

Objective function:

$$Max(Min(u_i)), \forall t_k \in T, \forall o_i \in O \tag{13}$$

The objective function of the proposed mechanism is to maximize the minimal *QoM* at each time slot for a given set of sensors S and the *POIs* O while maintaining the perpetual lifetime of WSNs. Some constraints given below should be satisfied.

Exp. (14) gives the *state constraint* which ensures that each sensor can stay in one of the four possible states, including *sensing-only*, *recharging-only, sensing* & *recharging* and *sleeping state,* at any given time.

1) STATE CONSTRAINT

$$\left(\alpha_{j,k}^{sen} + \alpha_{j,k}^{slp}\right) \leq 1 \text{ and } \left(\alpha_{j,k}^{rec} + \alpha_{j,k}^{slp}\right) \leq 1, \forall j, \forall k \tag{14}$$

Recall that each cycle is denoted by T. The following active constraint guarantees that the summation of numbers of the active sensors in all time slots of a cycle is equal to or smaller than the total number of the sensors in the entire network.

2) ACTIVE CONSTRAINT

$$\sum_{t_k \in T} \alpha_{j,k}^{sen} \leq |S|, \forall s_j \in S \tag{15}$$

As shown in Exp. (16), the energy constraint guarantees that the energy consumption of the sensor during the network lifetime is less than or equal to the energy harvested by the solar power. This constraint guarantees the perpetual lifetime of each sensor.

3) ENERGY CONSTRAINT

$$\sum_{t_k \in T} \left((e_{j,k} + e^{rec})\alpha_{j,k}^{rec}\right) \geq \left(e^{sen} + e^{rpt}\right)\alpha_{j,k}^{sen} \forall s_j \in S \tag{16}$$

The following section presents the proposed scheduling algorithm which aims to achieve our objective function given in (13) while satisfying the constraints (14), (15) and (16).

IV. THE PROPOSED SCHEDULING ALGORITHM

This paper presents two scheduling approaches to the sensors, called *Centralized Target Coverage Mechanism* (*C-MMQT)* and *Distributed Target Coverage Mechanism* (*D-MMQT*). The *C-MMQT* is executed in the base station which should collect all information about the sensors and targets, including their locations and the weight of each target. Then the scheduling results are delivered to the corresponding sensors. Alternatively, applying the *D-MMQT*, each sensor exchanges its location information with neighbors, makes the decision for its own schedule, and then notifies its schedule to the neighboring sensors. Although the *C-MMQT* mechanism can schedule the sensors with complete information, it has disadvantages including time and energy consumptions for data collection and scheduling result notification, as well as high computational complexity, as compared with the *D-MMQT.* The following presents the details of the proposed *MMQT* mechanisms.

A. C-MMQT MECHANISM

The proposed *C-MMQT* mechanism assumes that the locations of all sensors and *POIs* are known. The proposed *C-MMQT* mechanism consists of two phases: *Network Initialization Phase* (*NI Phase*) and *Scheduling Phase* (*SC Phase*). In the *NI Phase*, the length of each cycle and the detection probability of each sensor to each *POI* should be calculated. In the *SC Phase*, the sensors will be scheduled one by one according to current cooperative sensing probability.

1) PHASE I: NETWORK INITIALIZATION (NI PHASE)

In the *NI Phase*, the length of each cycle should be firstly calculated. This paper uses the ratio between the recharge and discharge times as its work period. For example, if there is a sensor that uses two time slots to recharge its battery 50J, that 50J can support the sensor to cover *POIs* only for a single time slot. That is to say, a sensor can recharge 25J for each time slot in the recharging-only state, but it consumes 50J for a single time slot in the sensing-only state. Therefore, the ratio between the recharge and discharge time is 2/1 and the length of each cycle for all sensors is 2+1. The sensors can only monitor the *POIs* for one time slot and have to recharge its battery in the other two time slots to guarantee that the sensor satisfies a perpetual lifetime. Assume that there are σ cycles for the entire day. Among them, there are β cycles in the daytime and $\sigma - \beta$ cycles in the nighttime.

The sensors have to reserve some energy recharged in the daytime to monitor the *POIs* in the nighttime since the sensors are solar-powered and they cannot recharge their battery in the nighttime. Let notation e^{night} denote the reserved energy of the sensors for the nighttime. Assume that the reserved energy e^{night} can support the energy consumption during the nighttime. Therefore, the reserved energy e^{night} have to be greater than or equal to the energy consumption of the sensors during the nighttime. That is,

$$(\sigma - \beta)(e^{sen} + e^{rpt}) \leq e^{night} \tag{17}$$

Hence, the sensors cannot utilize all of the energy e^{max} in the daytime. They have to deduct the reserved energy e^{night}, and the energy required for sensors to activate its solar panel e^{min}. As a result, the energy that a sensor can utilize in the daytime is shown in Exp. (18).

$$\beta(e^{max} - e^{min}) - e^{night} \tag{18}$$

In terms of recharging-only state, in order to make sure that the energy consumption and harvesting is balancing, the sensors have to supply the energy which was consumed and apportion the reserved energy e^{night} during each cycle in the daytime. The required energy of each sensor during each cycle in the daytime is shown in Exp. (19).

$$\frac{\beta(e^{max} - e^{min}) - e^{night}}{\beta} \tag{19}$$

When the base station completes the calculation of the energy consumption and the energy supplement of each sensor during a cycle, it will calculate the recharging and discharging times. The energy consumption of sensors in each cycle is $e^{sen} + e^{rpt}$. Let $\varphi^{daytime\_sen}$ denote the number of time slots that sensors can monitor the *POIs* in the daytime. The value of $\varphi^{daytime\_sen}$ can be calculated by applying Exp. (20).

$$\varphi^{daytime\_sen} = \left\lfloor \frac{\beta(e^{max} - e^{min}) - e^{night}}{e^{sen} + e^{rpt}} \right\rfloor \tag{20}$$

The energy supplement of sensors of a time slot in the recharging-only state is $e^{rec} - e^{min}$. Therefore, the number of time slots that sensors have to recharge its battery in the daytime is shown in Exp. (21).

$$\varphi^{daytime\_rec} = \left\lceil \frac{\beta(e^{max} - e^{min}) - e^{night}}{e^{rec} - e^{min}} \right\rceil \tag{21}$$

In the daytime, the proposed *C-MMQT* mechanism will use the ratio of recharging time $\varphi^{daytime\_rec}$ and discharging time $\varphi^{daytime\_sen}$ to calculate the length of one cycle. Let notation $\gamma^{daytime}$ be the ratio of recharging time and discharging time. The $\gamma^{daytime}$ can be calculated by applying Exp. (22).

$$\gamma^{daytime} = \left\lceil \frac{\varphi^{daytime\_rec}}{\varphi^{daytime\_sen}} \right\rceil \tag{22}$$

The value of $\gamma^{daytime}$ can be derived by applying the following expression.

$$T = \gamma^{daytime} + 1 \tag{23}$$

Fig. 4 depicts the relation of cycles in the daytime and nighttime. Recall that τ denotes the length of time slot. According to the recharging and discharging model, the length of e^{sen} is τ and the length of e^{rec} is $\kappa\tau$. Let $\mathbb{L}$ denote the length of a whole day. One day can be divided into two intervals: daytime and nighttime which are denoted by L^{day} and L^{night} respectively. Obviously, we have $\mathbb{L} = L^{day} + L^{night}$ and they can be partitioned into a number of equal-length slots as shown in Fig. 4.

Recall that notation e^{night} denotes the energy consumption of sensors in the nighttime. The number of time slots that

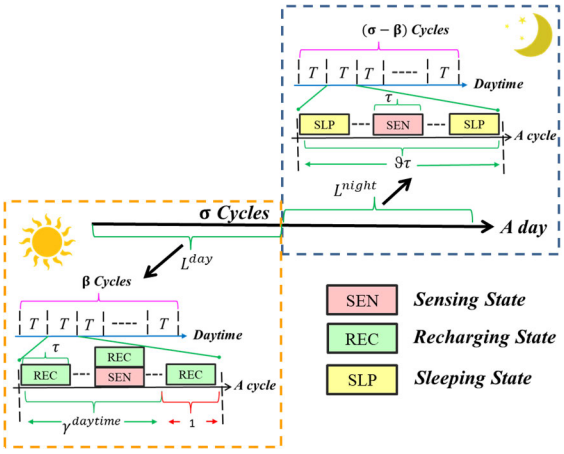

FIGURE 4. A cycle of daytime and nighttime.

sensors can monitor the *POIs* in the nighttime is shown in Exp. (24). The base station will divide the nighttime into $\gamma^{nighttime\_sen}$ cycles. Each sensor only can monitor the *POIs* in one of the time slots in a cycle and remain in the sleeping state in rest of the time slots to make sure that the total energy consumption in the nighttime is the reserved energy e^{night}.

$$\gamma^{nighttime\_sen} = \left\lfloor \frac{e^{night}}{e^{sen} + e^{rpt}} \right\rfloor \tag{24}$$

After the *NI Phase*, the length of one cycle have been calculated. Then the *SC Phase* will further schedule the sensors in one cycle to achieve the maximal *QoM* of the lowest target at any given time slot and to maintain the perpetual operation of the network.

2) PHASE II: SCHEDULING PHASE (SC PHASE)

In the *SC Phase*, the base station will schedule the sensors for one cycle in the daytime and then in the nighttime separately.

In this phase, there are three main tasks. First, the base station will find the space time points which have the smallest value. Second, it will find the sensors which can maximize the space time point that have the smallest value. Finally, it will schedule one best sensor from the unscheduled sensors. The above mentioned three tasks will be repeatedly performed until all sensors have been scheduled in the cycle. In the following, the three tasks will be described.

a: TASK 1: IDENTIFYING THE "BOTTLENECK SPACE TIME POINT"

This task aims to identify the bottleneck space time point of the newly selected *POI* such that the cooperative detection probability can be maximized.

To present the operations of this task, two matrices, including the $\mathcal{M}^{sch}_{m\times\eta}$ and $\mathcal{M}^{QoM}_{m\times\eta}$, will be introduced. Let $\mathcal{M}^{sch}_{m\times\eta}$ be a two-dimensional space time scheduling matrix where m denotes the number of targets and η denotes the cycle length. Each element $\mathcal{M}^{sch}[i, j]$ in $\mathcal{M}^{sch}$ denotes the set of sensors which have been scheduled to monitor *POI* $o_i \in O$ at time

slot $t_j \in T$. The space time matrix will be adopted to present the current scheduling results of each *POI* $o_i \in O$ at time slot $t_j \in T$.

Based on the scheduling of the current space time scheduling matrix $\mathcal{M}^{sch}$, each *POI* $o_i \in O$ will have a *QoM* value at each time slot $t_j \in T$. Let $\mathcal{M}^{QoM}_{m\times\eta}$ denote a two dimensional space time *QoM* matrix where m denotes the number of targets and η denotes the cycle length. Each element $\mathcal{M}^{QoM}[i,j]$ in $\mathcal{M}^{QoM}$ denotes the *QoM* value of space time point of *POI* $o_i \in O$ at time slot $t_j \in T$. The space time *QoM* matrix will be adopted to present the *QoM* value of each *POI* $o_i \in O$ at time slot $t_j \in T$ of the current scheduling.

Let $q_{i,j}$ denote the *QoM* value of element $\mathcal{M}^{QoM}[i,j]$. The value of $q_{i,j}$ can be calculated by applying Exp. (25).

$$q_{i,j} = 1 - \prod_{s_k \in \mathcal{M}^{sch}[i,j]} \left(1 - p\left(s_k, o_i\right)\right) \tag{25}$$

Let $q^{weak}_{i,j}$ denote the smallest value in $\mathcal{M}^{QoM}[i,j]$. That is,

$$q^{weak}_{i,j} = \underset{q_{i,j}\in M^{QoM}[i,j]}{Min} q_{i,j} \tag{26}$$

Let (o_i, t_j) denote the space time point which is the coordinates of $\mathcal{M}^{QoM}$ associated with *POI* o_i at time slot t_j. This task aims to identify the bottleneck space time point which has the smallest *QoM* value in $\mathcal{M}^{QoM}$.

In this task, the base station will find the space time points which have the smallest *QoM* value. Let (o^{weak}_i, t^{weak}_j) denote the *weakest space time point* corresponding to $q^{weak}_{i,j}$. Let ST^{weak} denote the set of all weakest space time points. We have

$$ST^{weak} = \{(o^{weak}_i, t^{weak}_j) | \mathcal{M}^{QoM}[i,j] = q^{weak}_{i,j}\} \tag{27}$$

According to Exp. (27), this task can identify the set ST^{weak} of all weakest space time points.

In the next two tasks, the base station will schedule one sensor which has the largest contribution to the bottleneck space time point, in terms of *QoM*.

b: Task 2: Selecting the Best Sensor for the "Bottleneck"

This task aims to select the best sensor from the unscheduled sensor set to improve the cooperative detection probability of the weakest space time points $(o^{weak}_i, t^{weak}_j) \in ST^{weak}$.

Let S^{sch} denote the set of scheduled sensors. The value of S^{sch} is shown in Exp. (28).

$$S^{sch} = \bigcup_{\substack{1 \le i \le m \\ 1 \le j \le \lambda}} M^{sch}[i,j] \tag{28}$$

Let S^{un_sch} denote the set of all unscheduled sensors. The set of S^{un_sch} can be calculated by using the following equation.

$$S^{un\_sch} = S \setminus S^{sch} \tag{29}$$

The base station is responsible for repeatedly performing this task until all the sensors which have a contribution to $(o^{weak}_i, t^{weak}_j) \in ST^{weak}$ have been scheduled. Let $\wp^{weak}$ denote the weakest space time point obtained from the first task. That is,

$$\wp^{weak}_{i,j} = \left(o^{weak}_i, t^{weak}_j\right), \forall \wp^{weak}_{i,j} \in ST^{weak} \tag{30}$$

Recall that this task aims to find the best sensor to be scheduled to maximize the *QoM* of current $\mathcal{M}^{QoM}$. Consider each unscheduled sensor $s_x \in S^{un\_sch}$. The next issue is to evaluate the contribution to the *QoM* of current $\mathcal{M}^{QoM}$ if sensor s_x is scheduled.

Let $b^{weak}_{i,j,x}$ denote the benefit of the sensor s_x monitoring o_i at t_j. The value of $b^{weak}_{i,j,x}$ can be calculated by applying Exp. (31).

$$b^{weak}_{i,j,x} = 1 - \prod_{s_j \in \mathcal{M}^{sch}[i,j] \cup \{s_x\}} \left(1 - p\left(s_j, O_i\right)\right) - q_{i,j} \tag{31}$$

Let $\rho_{i,j}$ be a Boolean variable representing whether or not $\wp^{weak}_{i,j}$ belongs to ST^{weak}. That is,

$$\rho_{i,j} = \begin{cases} 1 & \text{if } \wp^{weak}_{i,j} \in ST^{weak} \\ 0 & \text{otherwise} \end{cases}. \tag{32}$$

Let $B^{weak}_{i,j,x}$ denote the total benefit of the sensor s_x to all weakest space time points in ST^{weak}.

$$B^{weak}_{i,j,x} = \sum\nolimits_{o_i \in O_x} b^{weak}_{i,j,x} \cdot \rho_{i,j} \tag{33}$$

Similarly, let $B^{non\_weak}_{i,j,x}$ denote the total benefit of the sensor s_x to all space time points not in ST^{weak}. We have

$$B^{non\_weak}_{i,j,x} = \sum\nolimits_{o_i \in O_x} b^{weak}_{i,j,x} \cdot (1 - \rho_{i,j}) \tag{34}$$

Let O_x denote the set of targets covered by a sensor s_x. The total benefit of the sensor s_x to the *QoM* of all targets $o_i \in O$.

$$B_{i,j,x} = \omega \left(B^{weak}_{i,j,x}\right) + (1 - \omega) B^{non-weak}_{i,j,x} \tag{35}$$

where ω is the weight for combining two benefits $B^{weak}_{i,j,x}$ and $B^{non-weak}_{i,j,x}$.

Let $B^{best}_{i,j}$ be the maximal benefit of the weakest space time point (o^{weak}_i, t^{weak}_j) obtained by considering all possible $s_x \in S_i$. We have

$$B^{best}_{i,j} = \max_{s_x \in s_i} B_{i,j,x} \tag{36}$$

Let $s^{best}_{i,j}$ denote the best sensor that has the largest contribution to weakest space time point (o^{weak}_i, t^{weak}_j). The $s^{best}_{i,j}$ can be derived by applying Exp. (37).

$$s^{best}_{i,j} = \arg\max_{s_x \in s_i} B_{i,j,x} \tag{37}$$

The above $s^{best}_{i,j}$ is the best sensor for improving the certain weakest space time point $\wp^{weak}_{i,j} \in ST^{weak}$. Since there might be more than one $\wp^{weak}_{i,j}$ in ST^{weak}, the weakest space time point that could obtain maximal benefit from the help of $s^{best}_{i,j}$ should be identified. Consequently, the best sensor to be scheduled for improving the maximal *QoM* of the current

weakest space time points $\wp_{i,j}^{weak} \in ST^{weak}$ can be derived by applying Exp. (38).

$$s^{best} = arg \max_{\wp_{i,j}^{weak} \in ST^{weak}} B_{i,j}^{best} \tag{38}$$

Let $B_{\hat{i},\hat{j}}^{best}$ be the maximal benefit obtained by comparing all schedules to the weakest space time point in ST^{weak}. We have

$$B_{\hat{i},\hat{j}}^{best} = \max_{\wp_{i,j}^{weak} \in ST^{weak}} B_{i,j}^{best} \tag{39}$$

Let $\wp_{\hat{i},\hat{j}}^{weak}$ be the best space time point which can obtain the maximal benefit from the help of s^{best}. We have

$$\wp_{\hat{i},\hat{j}}^{weak} = arg \max_{\wp_{i,j}^{weak} \in ST^{weak}} B_{i,j}^{best} \tag{40}$$

According to the Exp. (40), the base station selects the s^{best} from the S^{un_sch} to monitor the space time point

$$\wp_{\hat{i},\hat{j}}^{weak} = (o_{\hat{i}}^{weak}, t_{\hat{j}}^{weak})$$

If there is more than one sensor which can maximize the cooperative detection probability of $o_{\hat{i}}^{weak}$ at $t_{\hat{j}}^{weak}$, the base station will select the best sensor s^{best} to monitor the target $o_{\hat{i}}^{weak}$ at time slot $t_{\hat{j}}^{weak}$ for obtaining the maximal benefit of surveillance quality. In the following task, the base station will schedule a sensor s^{best} to the bottleneck space time point.

c: TASK 3: SCHEDULING THE SENSOR FOR THE "BOTTLENECK"

This task schedules the best sensor s^{best} obtained in the second task to monitor the weakest space time point for improving its cooperative detection probability. First, the s^{best} should join the space time scheduling matrix. That is,

$$\mathcal{M}^{sch}\left[\hat{i},\hat{j}\right] = \mathcal{M}^{sch}\left[\hat{i},\hat{j}\right] \cup \{s^{best}\} \tag{41}$$

All elements in the $\hat{j}$-*th* column of space time *QoM* matrix should be updated accordingly, as shown in Exp. (42).

$$\mathcal{M}^{QoM}\left[\hat{i},\hat{j}\right] = q_{\hat{i},\hat{j}} = 1 - \prod\nolimits_{s_k \in \mathcal{M}^{sch}\left[\hat{i},\hat{j}\right]} \left(1 - p\left(s_k, o_{\hat{i}}\right)\right) \tag{42}$$

for each $o_{\hat{i}}$ in the coverage of s^{best}. After that, the s^{best} should be removed from S^{un_sch}. That is,

$$S^{un\_sch} = S^{un\_sch} \setminus \{s^{best}\} \tag{43}$$

The sensor s^{best} also needs to be included in the set S^{sch} of scheduled sensors.

$$S^{sch} = S^{sch} \cup \{s^{best}\} \tag{44}$$

The new weakest space time point should be re-identified by applying Exp. (27). The base station will repeatedly perform the three tasks designed in this phase until all the sensors have been scheduled.

Fig. 5 gives an example of selecting the best sensor to improve the *QoM* of the weakest space time point. Assume

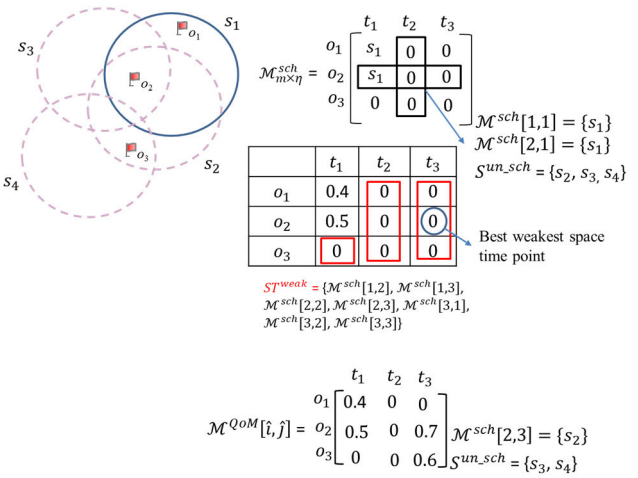

FIGURE 5. An example of selecting the best sensor s_2 to improve the QoM of space time point $\wp_{\hat{i},\hat{j}}^{weak}=(o_2^{weak}, t_3^{weak})$.

that $S = \{s_1, s_2, s_3, s_4\}$ is the set of sensors and $O = \{o_1, o_2, o_3\}$ is the set of *POIs*. Each sensor $s_i \in S$ calculates its detection probability to o_1, o_2 and o_3 by applying Exp. (31). As shown in Fig. 5, there is a set of weakest space time points shown in ST^{weak}. To schedule the sensor s_4 for monitoring $\wp_{\hat{i},\hat{j}}^{weak} = (o_3^{weak}, t_1^{weak})$, it has very small contribution to the *POIs* o_1 and o_2 because of its cooperative detection probability. But sensor s_2 has a large contribution to the *POIs* o_2 and o_3, as compared to the sensor s_4. Therefore sensor s_2 is selected as the best sensor to improve the best weakest space time point $\wp_{\hat{i},\hat{j}}^{weak} = (o_2^{weak}, t_3^{weak})$. Hence, the values in the $\mathcal{M}^{QoM}$ [2, 3] and $\mathcal{M}^{QoM}$ [3, 3] are updated according to the schedule of sensors.

Though the proposed centralized algorithm *C-MMQT* can efficiently schedule all sensors aiming to maximize the *QoM* of the target with the minimal *QoM*, it assumes that the information of all sensors and *POIs* are known to each sensor. The following subsection further presents a distributed algorithm, called *D-MMQT*, which only needs to maintain the local information for each sensor.

B. D-MMQT MECHANISM

This section proposed a distributed scheduling algorithm, called *D-MMQT*. Assume that each sensor is only aware of the information of its neighbors. All sensors are clock synchronized. There are several challenges when designing *D-MMQT*. The first challenge is that the local information maintained by all nodes might be different, even though they are neighbors. The contradiction among local decisions made by neighbors might exist. To cope with this problem, *D-MMQT* should guarantee that the larger benefit of the local decision will be the final decision when the decisions exist contradiction. Second, the broadcast packets containing the local decisions might have collisions. The *D-MMQT* should avoid collision occurrence. To cope with the decision-contradiction

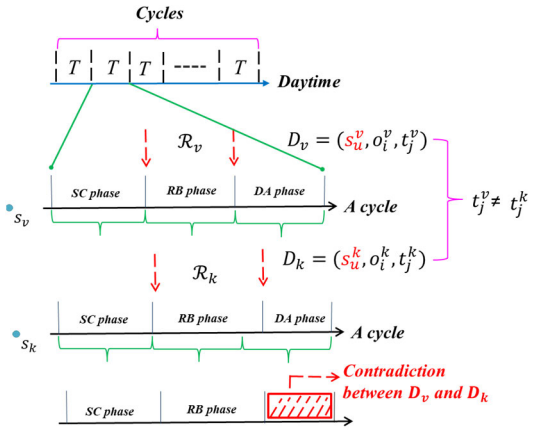

FIGURE 6. An example of three phases of D-MMQT.

and packet collision problems, the proposed *D-MMQT* mechanism consists of three phases: *Scheduling Phase* (*SC Phase*), *Random Back-off Phase (RB Phase)* and *Decision Announcement Phase* (*DA Phase*), as shown in Fig. 6. In the SC phase, each sensor identifies the weakest space time point and selects the best sensor to improve the *QoM* of the weakest space time point based on its local information.

In the RB phase, each sensor waits for a back-off time based on the contribution of its scheduling decision. After waiting for the back-off time, each sensor enters the DA phase which broadcasts its decision to notify its neighbors. All neighbors will update its space time *QoM* and space time scheduling information according to the received decision from neighbors. The following presents the details of each phase.

1) PHASE I: SCHEDULING (SC PHASE)

Each sensor, say s_v, in *SC phase* should perform four tasks. The first task is to calculate the probability of each neighboring sensor to each target covered by s_v. Let O_v denote the set of targets in the sensing range of sensor s_v. Let N_v denote the set of neighbors of sensor s_v. That is,

$$N_v = \{s_i | d(s_i, s_v) < r_c\}, s_v \in S \tag{45}$$

Let l_i^{sensor} and l_j^{target} denote the locations of neighbor $s_i \in N_v$ and target $o_j \in O_v$, respectively. Based on the information including locations l_i^{sensor} of all neighbors $s_i \in N_v$ and locations l_j^{target} of all targets $o_j \in O_v$, the probability $P(s_i, o_j)$ can be calculated by applying Exp. (1).

The second task is to calculate the cycle time which can be calculated by applying Exps. (20), (21), (23) and (24). The third task is to find the weakest space time point. Similar to the global matrices $\mathcal{M}_{m\times\eta}^{sch}$ and $\mathcal{M}_{m\times\eta}^{QoM}$ as defined in *SC* phase of *C-MMQT* approach, we define that $\mathcal{M}_{m_v\times\eta_v}^{sch,v}$ and $\mathcal{M}_{m_v\times\eta_v}^{QoM,v}$ denote *the local space time scheduling* and *QoM matrices* of sensor s_v, respectively, where m_v denotes the number of targets covered by s_v and η_v denotes the cycle length. Let $q_{i,j}^v$ denote the *QoM* value of an element $M^{QoM,v}[i,j]$. Let $q_{i,j}^{weak,v}$ denote the smallest value in $\mathcal{M}^{QoM,v}[i,j]$. That is,

$$q_{i,j}^{weak,v} = \underset{q_{i,j}^v \in \mathcal{M}^{QoM,v}[i,j]}{Min} q_{i,j}^v \tag{46}$$

Similarly, let $\wp_{i,j}^{weak,v} = (o_i^v, t_j^v)$ denote the *weakest space time point* corresponding to $q_{i,j}^{weak,v}$ and $ST^{weak,v}$ denote the set of all weakest space time points. We have

$$ST^{weak,v} = \{(o_i^v, t_j^v) | \mathcal{M}^{QoM,v}[i,j] = q_{i,j}^{weak,v}\} \tag{47}$$

Let $D_v = (s_u^v, o_i^v, t_j^v)$ denote the decision made by a sensor s_v, which schedules sensor $s_u \in N_v \cup s_v$ to monitor the weakest space time point $\wp_{i,j}^{weak,v} = (o_i^v, t_j^v)$. According to Exp. (38), the best sensor s_u^v in D_v can be derived. Similarly, the weakest space time point $\wp_{i,j}^{weak,v} = (o_i^v, t_j^v)$ can be derived according to Exp. (40). Let B_v denote the benefit obtained from the decision D_v. The value of B_v can be derived according to Exp. (39).

2) PHASE II: RANDOM BACK-OFF PHASE (RB PHASE)

In the *RB Phase*, each sensor waits for a random time. Two major reasons for applying the random back-off policy in the second phase. First, the decisions $D_k = (s_u^k, o_i^k, t_j^k)$ of neighbors $s_k \in N_v$ might contradict to the decision $D_v = (s_u^v, o_i^v, t_j^v)$ made by a sensor s_v. The design of random back-off policy should guarantee that the better decision should be announced earlier and the worse decision should be given up accordingly. Another important reason for applying the random back-off policy is to avoid packet collisions occurred among neighbors. To cope with the contradiction problem and guarantee that better decision should be adopted, the waiting time of each sensor s_v should be determined according to the contribution of its own decision. Let R_v denote the random back-off time of the sensor s_v. Since the random back-off time should guarantee two criteria: (1) decision with larger benefit should be announced earlier and (2)collision avoidance, the value of $\mathcal{R}_v$ can be determined by applying Exp. (48).

$$\mathrm{R}_v = 1/(|N_v| \times B_v) \tag{48}$$

It indicates that R_v is inversely proportional to the benefit B_v and the number of neighbors of sensor s_v. All the sensors would countdown from its back-off time to 0. As shown in Fig. 6, sensors s_v and s_k have made their decisions D_v and D_k, respectively. However, the two decisions contradict to each other because both of them schedule the same neighboring sensor s_u to work in different time slots ($t_j^v \neq t_j^k$). In this example, s_k has a larger random back-off value than s_v because that D_v leads to a larger benefit than D_k. During the random back-off period, if s_v receives the decision $D_k = (s_u^k, o_i^k, t_j^k)$ from its neighbor s_k, it will check if its own decision $D_v = (s_u^v, o_i^v, t_j^v)$ contradicts to the received decision $D_k = (s_u^k, o_i^k, t_j^k)$. If it is the case, sensor s_v will give up its decision. Otherwise, the sensor s_v can still keep its decision and wait for the counter R_v achieving zero for broadcasting its decision. Herein, it is noticed that no matter

whether or not decisions D_v and D_k have a contradiction, all sensors which have received the decision D_k should update its space time scheduling and *QoM matrices* according to decision $D_k = (s_u^k, o_i^k, t_j^k)$. Continue the example shown in Fig. 6, Sensor s_k should give up its decision D_k in the next phase.

The following presents the check conditions for identifying if the contradiction existed between two decisions D_v and D_k. Let $\xi_{sensor}^{i,v}$ be the Boolean variable representing whether or not s_u^i is equal to the s_u^v. That is,

$$\xi_{sensor}^{v,k} = \begin{cases} 1 & \text{if } s_u^v = s_u^k \\ 0 & \text{otherwise} \end{cases} \tag{49}$$

Similarly, let $\psi_{time}^{v,k}$ denote the Boolean variable representing whether or not t_j^v is equal to t_j^k. That is,

$$\psi_{time}^{v,k} = \begin{cases} 0 & if\ t_j^v = t_j^k \\ 1 & if\ t_j^v \neq t_j^k \end{cases} \tag{50}$$

Decisions D_v and D_k exist contradiction if the following condition holds.

$$\xi_{sensor}^{v,k} \times \psi_{time}^{v,k} = 1 \tag{51}$$

This occurs because of that sensors s_v and s_k schedule the same sensor s_u to monitor certain targets at different time slots. In case that Condition (51) holds, sensor s_v should give up its decision and then update its scheduling and *QoM matrices* according to decision D_k.

3) PHASE III: DECISION ANNOUNCEMENT PHASE (DA PHASE)

In the *DA Phase,* each sensor simply broadcasts its decision which is made in *SC phase* and updates its scheduling matrix.

V. PERFORMANCE EVALUATION

This section evaluates the performance improvement of the proposed *C-MMQT*, *D-MMQT* against the existing Quality Aware Target Coverage Mechanisms (*C-QATC, D-QATC*) and Greedy Hill-Climbing Activation Scheme (*GHCAS*). The *QATC* algorithm [14] aimed to schedule different subsets of sensors. Each sensor set was activated in some certain time slot, which leads to the situation that different subsets of targets can be covered at some certain time slots. The *GHCAS* algorithm [15], is presented to address the utility based target coverage problem by scheduling a sensor into a time-slot to maximize the incremental utility together with the sensor which is previously scheduled. The following firstly illustrates the simulation environment and then presents the simulation results.

A. SIMULATION MODEL

The simulation parameters are given in Table 2. In the experimental study, the MATLAB is used as the simulation tool. The sensor nodes and the *POIs* are randomly deployed in the monitoring area as shown in Fig. 7. The size of the monitoring region is $400m \times 400m$ while the number of deployed sensors is ranging from 500 to 2000. The communication radius is 20m while the sensing radius is 10m. The guarantee sensing range for sensor detection is 5m. Let e^{max} and e^{min} denote the initial energy and the energy consumption of sensors to activate its solar panel, which is set at 1210 Joule and 10 Joule respectively. The recharging and discharging rates of the solar battery is 25 Joule/hour and 50 Joule/hour, respectively. That is to say, the ratio of recharging over discharging time periods is 2, and the cycle length is 3 time slots.

TABLE 2. Simulation settings.

Parameters	Values
Simulator	Matlab
Node deployment	Random
Monitoring region	400 $m \times 400$ m
Number of sensors	500 – 2000
Sensing Radius	10 m
Guarantee Sensing Radius	5m
Communication Radius	20 m
e^{max}	1210 Joule
e^{min}	10 Joule
Recharging rate	25 Joule/hour
Discharging rate	50 Joule/hour

B. SIMULATION RESULTS

Fig. 8 compares the quality of monitoring of the five algorithms by varying the number of sensors and the number of *POIs*. The number of sensors is varied ranging from 500 to 2000 while the number of *POIs* is varied ranging from 20 to 110. As shown in Fig. 8, the monitoring qualities of the five compared algorithms significantly increase with the number of sensors. This occurs because more sensors can participate in the monitoring task in each time slot, leading to a high quality of monitoring. On the other hand, the monitoring qualities of five algorithms generally decrease with the number of *POIs.* It occurs because when the number of *POIs* is increased, more sensors are required to monitor each *POIs*. In comparison, the proposed *C-MMQT* outperforms the other four algorithms in terms of quality of monitoring and almost achieves 1 when the number of deployed sensors is 2000 and the number of *POIs* is 20. This occurs because that the proposed *C-MMQT* applies PSM and selects the sensor with the largest contribution to improve the quality of each bottleneck space time point. As a result, the *C-MMQT* achieves the best performance as compared with the other four existing algorithms.

Fig. 9 further investigates the average utility of *C-MMQT, C-QATC, D-MMQT*, *D-QATC* and *GHCAS* by varying the number of *POIs.* The number of sensors varies from 500 to 1500 and the number of *POIs* varies ranging from 20 to 110. Let *A* (*1500*), *A* (*1000*) and *A* (*500*) denote the 1500 sensors,

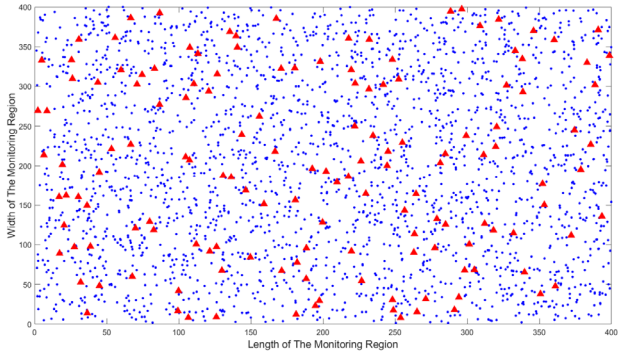

FIGURE 7. A scenario that sensors and POIs are randomly deployed in a monitoring area with size 400m∗400m.

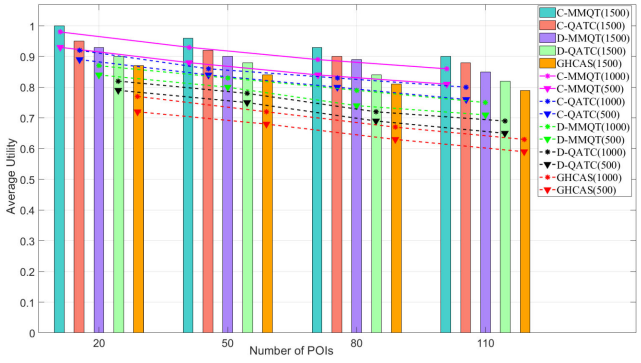

FIGURE 9. Comparison of C-MMQT, C-QATC, D-MMQT, D-QATC and GHCAS in terms of average utility by varying the number of POIs.

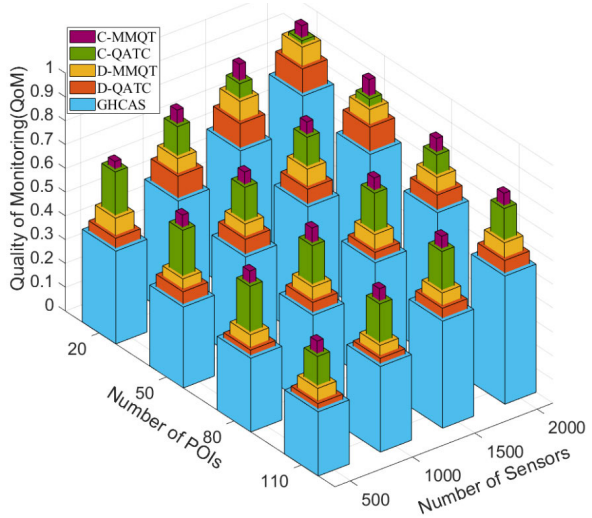

FIGURE 8. Comparison of C-MMQT, C-QATC, D-MMQT, D-QATC and GHCAS in terms of monitoring quality by varying the number of sensors and the number of POIs.

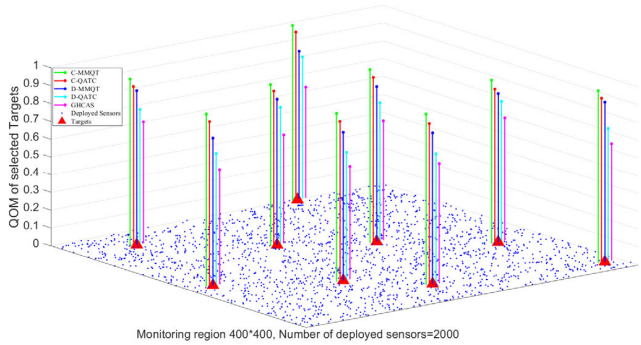

FIGURE 10. Comparison of C-MMQT, C-QATC, D-MMQT, D-QATC and GHCAS in terms of quality of monitoring by selecting the targets.

1000 sensors and 500 sensors deployed by applying algorithm A, respectively, where A can be *C-MMQT*, *C-QATC, D-MMQT, D-QATC* and *GHCAS*. The average utility is defined as the utility achieved per target per time slot. As shown in Fig. 9, the average utility of the *C-MMQT* is better than those by applying *C-QATC, D-MMQT, D-QATC* and *GHCAS* algorithms. This occurs because the proposed *C-MMQT* adaptively finds the weakest space time point and schedule the best sensor to maximize the *QoM* of the weakest space time point. As a result, the proposed *C-MMQT* maximizes the quality of the target with the minimal quality. The average *QoM* achieved by the proposed *C-MMQT* is 0.9987. When the number of deployed sensors is 1500, the achieved average *QoM* is larger than 0.9 in all cases. Finally, when the number of sensors is 500, the average *QoM* is no less than 0.81.

Fig. 10 further compares the *QoM* of randomly selected 9 targets by applying the *C-MMQT*, *C-QATC, D-MMQT, D-QATC* and *GHCAS*. In the experiment, the area of the monitoring region is 400m $*$ 400m and the number of sensors is set in 2000. In comparison, the proposed *C-MMQT* algorithm outperforms the *C-QATC, D-MMQT, D-QATC* and *GHCAS* in terms of the quality of monitoring of randomly selected targets. This occurs because the proposed *C-MMQT* considers the bottleneck quality of monitoring of the targets and maximizes the minimal *QoM* of targets at any time slot and balance their *QoM* which results in high quality of monitoring. Besides, the *C-QATC, D-QATC* and *GHCAS* algorithms aim to maximize the overall coverage quality for the monitoring region. This policy might lead to the imbalanced *QoM* of each target at any given time because it is possible that a target with the minimal quality still remain with the lowest *QoM* while the other target with the highest quality obtains the *QoM* improvement.

Fig. 11 further studies the fairness indices of the compared five algorithms. The number of sensors is varied ranging from 500 to 2000 while the number of *POIs* ranging from 20 to 110. The *Fairness Index* $\zeta_{fairness}$ of quality of monitoring is defined as shown in Exp. (52). Let n denote the number of sensor nodes and x_i denote the quality of monitoring of sensor node s_i in each cycle.

$$\zeta_{fairness} = \frac{\left(\sum_{i=1}^{n} x_i\right)^2}{n \sum_{i=1}^{n} x_i^2} \tag{52}$$

In comparison, the proposed *C-MMQT* outperforms the other four algorithms in terms of the fairness index. This

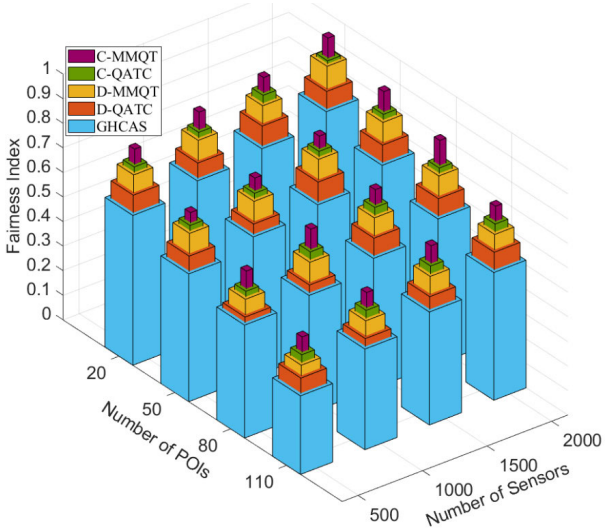

FIGURE 11. Comparison of C-MMQT, C-QATC, D-MMQT, D-QATC and GHCAS in terms of Fairness Index.

occurs because the *C-QATC, D-QATC* and *GHCAS* did not consider the importance of *POIs* and the lowest quality of the target. Therefore, in some time slots, some *POIs* are undetected which results in low fairness. The proposed *C-MMQT* considers the importance of *POIs*, finds the weakest space time points and schedules the best unscheduled sensor to improve the quality of the weakest space time point. Therefore, the fairness index of *C-MMQT* is close to 1.

Fig. 12 compares the fairness indices of *QoM* of 9 randomly selected targets. The observed locations are similar to those as shown in Fig. 10. The fairness index of quality of monitoring can be calculated for a given n time slots or given m locations. Let $q_{i,j}$ denote the quality of monitoring of j-th location at i-th time slot in one cycle. Let ζ_j and ζ_i denote the fairness indices of the j-th location for n time slots and the i-th slot on m locations respectively. The value of ζ_j and ζ_i is defined as shown in Exp. (53) and Exp. (54), respectively.

$$\zeta_j = \frac{\left(\sum_{i=1}^{n} q_{i,j}\right)^2}{n \sum_{i=1}^{n} q_{i,j}^2} \tag{53}$$

$$\zeta_i = \frac{\left(\sum_{j=1}^{m} q_{i,j}\right)^2}{n \sum_{j=1}^{m} q_{i,j}^2} \tag{54}$$

The fairness indices of the 9 randomly selected target locations being approximate to 1 which indicates that the quality of monitoring is stable. Fig. 12(a) compares the fairness indices of three time slots on 9 random locations. As shown in Fig. 12(a), the proposed *C-MMQT* outperforms the other four *C-QATC, D-MMQT, D-QATC,* and *GHCAS* algorithms in terms of fairness index and almost achieves 0.987 for all cases. This occurs because the *C-MMQT* considers the bottleneck *POIs* and allocates an unscheduled sensor to cooperatively monitor the bottleneck *POIs* with the lowest quality of monitoring. Similar to the results of Fig. 12(a), Fig. 12(b) depicts that the proposed *C-MMQT* outperforms the *C-QATC,*

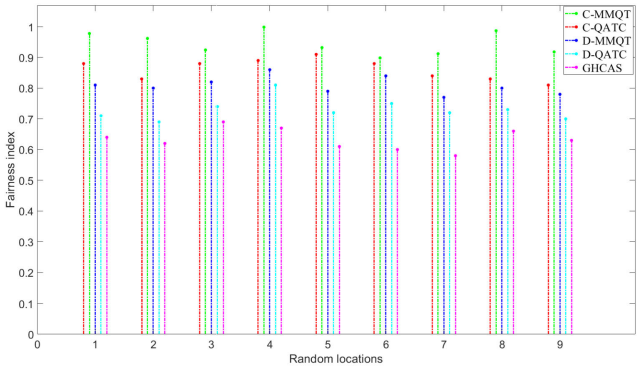

(a) Fairness index of observed target locations.

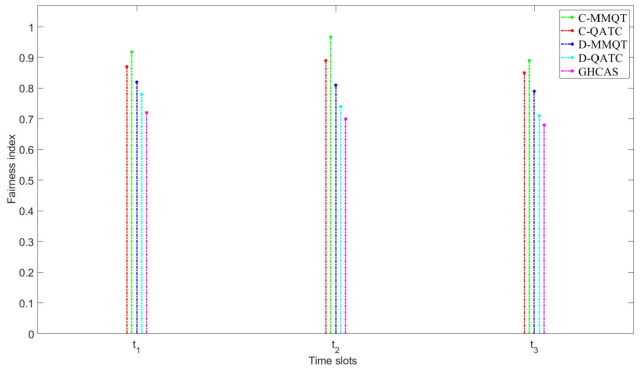

(b) Fairness index of observed time slots.

FIGURE 12. Performance comparison of the fairness index at 9 observed target locations and observed timeslots.

D-MMQT, D-QATC and *GHCAS* algorithms in terms of the fairness index for the observed time slots.

Fig. 13 compares the efficiency of the five compared algorithms by varying the number of sensors and the number of *POIs*. The number of sensors is varied ranging from 500 to 2000 whereas the number of *POIs* is varied ranging from 20 to 110. As shown in Fig. 13, the efficiencies of the five algorithms increase with the number of sensors and decrease with the number of *POIs.* The performance of the proposed *C-MMQT* is better as compared with the *C-QATC, D-MMQT, D-QATC* and *GHCAS* algorithms in most cases. This occurs because the proposed *C-MMQT* considers the *QoM* of each *POI*, which accurately evaluates the quality of monitoring of all the *POIs* in all the time slots. The proposed algorithm identifies the target with the lowest quality of monitoring and schedules a sensor in order to maximize its quality of monitoring. As a result, the quality of monitoring of all the *POIs* can be significantly increased, which leads to higher efficiency. However, when the number of *POIs* increases each sensor can monitor a higher number of *POIs* in each time slot. Therefore, the contribution of each sensor is high which leads to higher efficiency.

Fig. 14 investigates the quality of monitoring of *C-MMQT, C-QATC, D-MMQT, D-QATC* and *GHCAS* algorithms by varying the coverage range and the number of *POIs.* The number of sensors deployed in the monitoring region is 500.

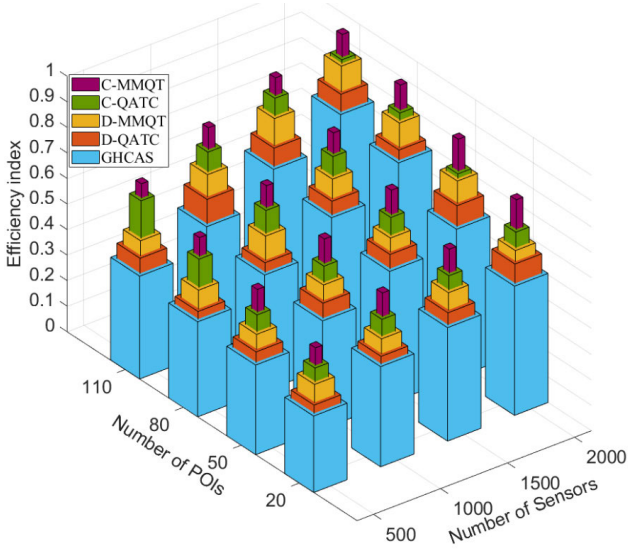

FIGURE 13. Comparison of C-MMQT, C-QATC, D-MMQT, D-QATC and GHCAS in terms of efficiency index by varying the number of sensors and the number of POIs.

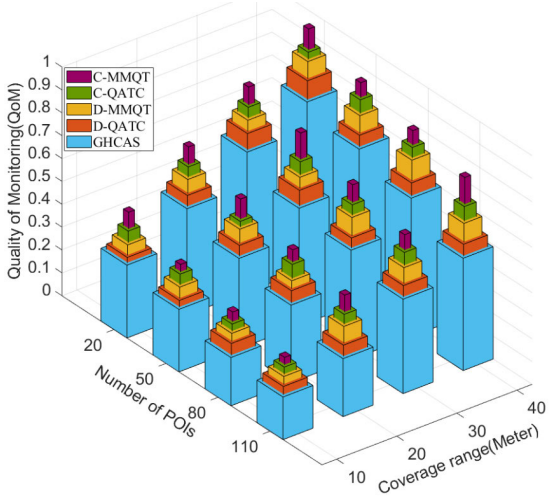

FIGURE 14. Comparison of C-MMQT, C-QATC, D-MMQT, D-QATC and GHCAS in terms of quality of monitoring by varying the coverage range and the number of POIs.

The coverage range of each sensor is set at 10m, 20m, 30m and 40m. The number of *POIs* is varied ranging from 20 to 110. As shown in Fig. 14, a common trend of five compared algorithms is that the *QoMs* of targets are increased with the coverage range of a sensor but are decreased with the number of *POIs*. This occurs because when the number of deployed sensors is fixed and the coverage range of sensor increases, each sensor can have a larger coverage area that can cover more *POIs*. Therefore, each *POIs* is much easier to be covered by any sensor which increases the quality of monitoring. On the other hand, the *QoMs* of targets decrease with the number of *POIs*. This occurs because when the number of sensors is fixed, some sensors should move to monitor the weakest time slot. Then all the other sensors have smaller monitoring opportunities when the number of *POIs* increases. Hence, all the other *POIs* have a lower quality of monitoring. In comparison, the proposed *C-MMQT* algorithm

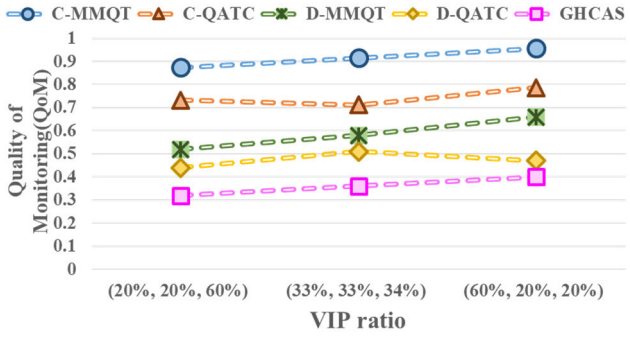

FIGURE 15. Comparison of C-MMQT, C-QATC, D-MMQT, D-QATC and GHCAS in terms of quality of monitoring vs VIP ratio.

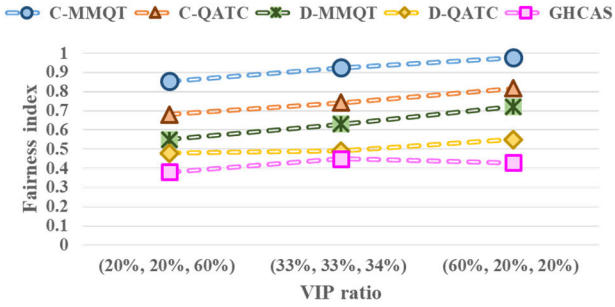

FIGURE 16. Comparison of C-MMQT, C-QATC, D-MMQT, D-QATC and GHCAS in terms of fairness index vs VIP ratio.

outperforms the other four algorithms in terms of the quality of monitoring. This occurs because that the proposed *C-MMQT* balances the *QoM* of each *POIs* at any given time and applies PSM to evaluate the sensing probability which can reflect the physical features of the sensing behavior which results in high quality of monitoring.

Fig. 15 further compares the quality of monitoring by varying the VIP ratio. The number of sensors and the number of *POIs* is set at 500 and 50, respectively. There are three types of different *POIs*: the low, middle and high importance of *POIs*. The VIP ratio represents the ratio of the number of each type of *PIOs* to the total number of *POIs*. For instance, VIP ratio = (20%, 20%, 60%) represents that the numbers of *types* 1 and 2 of *POIs* are equally (20%) while the number type 3 of *POIs* is 60%, as compared to the total number of *POIs*. The experimental results show that the *C-MMQT* outperforms the other four algorithms. This occurs because the *C-MMQT* considered the importance of *POIs* and always schedules the sensor to the *POIs* with higher importance. The third VIP ratio (60%, 20%, 20%) has a higher quality of monitoring when compared to the other two VIP ratios. The main reason is that when the *POIs* 1 is more important, some sensors which are monitoring the unimportant *POIs* will be scheduled to monitor *POIs* 1, leading to a high quality of monitoring of the proposed *C-MMQT*, as compared with the other four algorithms.

Fig. 16 compares the fairness index by varying the VIP ratio. The number of sensors and the number of *POIs* is set at 500 and 50, respectively. The experimental results show that the proposed *C-MMQT* has better fairness when compared

to the other four algorithms. A common trend as shown in Fig. 16 is that the fairness index gradually increases with the different VIP ratios. In the case of the first VIP ratio (20%, 20%, 60%), fairness is low when compared to the other VIP ratios. This occurs because when the number of sensors is fixed and the maximum number of sensors are scheduled to monitor *POIs* 3 results in low fairness. On the contrary, the fairness of the *C-QATC, D-QATC*, *GHCAS* algorithms is very low compared to the proposed algorithms. Regardless of the VIP ratio, the *C-QATC, D-QATC*, *GHCAS* algorithms schedule the sensors to monitors the *POIs*. Hence, some of the very important *POIs* are undetected in some time slots which results in low fairness.

VI. CONCLUSIONS

This paper proposes two efficient sensor activation schedules, called *C-MMQT* and *D-MMQT*, aiming at balancing the *QoM* of the *POIs* at any time slots by scheduling the solar-powered sensors. The proposed mechanisms apply the PSM by considering the importance of *POIs* and guarantees that all *POIs* can be well monitored at any given time slot. To maintain the sensor network with a perpetual lifetime, each sensor is carefully scheduled to maximize the minimal *QoM* of bottleneck *POIs* at any time slot. The proposed *C-MMQT* is a centralized approach that identifies the weakest space time point and schedules the sensor which has the maximal contribution for monitoring that point. On the contrary, the proposed *D-MMQT* is a distributed approach which only maintains the neighboring information and makes its own decision using the local information. Since the decisions among neighbors might contradict to each other, a random back-off policy is adopted based on the contributions of the local decisions. Experimental results show that the proposed *C-MMQT* achieves better performance than *C-QATC, D-MMQT, D-QATC* and *GHCAS* in all cases in terms of quality of monitoring.

The future work would relax the constraints of this paper and allow that sensors are partially recharged and with adjustable sensing range. Furthermore, we would like to study the heterogeneous sensor networks where different sensors have different charging and recharging pattern at the same time.

REFERENCES

[1] O. O. Ogundile, M. B. Balogun, O. E. Ijiga, and E. O. Falayi, "Energy-balanced and energy-efficient clustering routing protocol for wireless sensor networks," *IET Commun.*, vol. 13, no. 10, pp. 1449–1457, Jun. 2019.

[2] P. Nayak and A. Devulapalli, "A fuzzy logic-based clustering algorithm for WSN to extend the network lifetime," *IEEE Sensors J.*, vol. 16, no. 1, pp. 137–144, Jan. 2016.

[3] Y. Hong and X. Liu, "Extension of lifetime with network coding in cluster based wireless sensor networks," in *Proc. IEEE 2nd Adv. Inf. Technol., Electron. Autom. Control Conf. (IAEAC)*, Chongqing, China, Mar. 2017, pp. 1219–1223.

[4] J. K. Deepak Keynes and D. S. Punithavathani, "Clustering methodology to prolong lifetime in wireless sensor networks," in *Proc. Int. Conf. Inf. Commun. Embedded Syst. (ICICES)*, Chennai, India, Feb. 2017, pp. 1–8.

[5] V. Pal, G. Singh, and R. P. Yadav, "Balanced cluster size solution to extend lifetime of wireless sensor networks," *IEEE Internet Things J.*, vol. 2, no. 5, pp. 399–401, Oct. 2015.

[6] P. S. Lakshmi, M. G. Jibukumar, and V. S. Neenu, "Network lifetime enhancement of multi-hop wireless sensor network by RF energy harvesting," in *Proc. Int. Conf. Inf. Netw. (ICOIN)*, Chiang Mai, Thailand, Jan. 2018, pp. 738–743.

[7] S. Bi and R. Zhang, "Placement optimization of energy and information access points in wireless powered communication networks," *IEEE Trans. Wireless Commun.*, vol. 15, no. 3, pp. 2351–2364, Mar. 2016.

[8] W. Guowei, C. Lin, Y. Li, L. Yao, and A. Chen, "A multi-node renewable algorithm based on charging range in large-scale wireless sensor network," in *Proc. 9th Int. Conf. Innov. Mobile Internet Services Ubiquitous Comput.*, Blumenau, Brazil, Jul. 2015, pp. 94–100.

[9] W. Ejaz, M. Naeem, M. Basharat, A. Anpalagan, and S. Kandeepan, "Efficient wireless power transfer in software-defined wireless sensor networks," *IEEE Sensors J.*, vol. 16, no. 20, pp. 7409–7420, Oct. 2016.

[10] W. Ni and X. Dong, "Energy harvesting wireless communications with energy cooperation between transmitter and receiver," *IEEE Trans. Commun.*, vol. 63, no. 4, pp. 1457–1469, Apr. 2015.

[11] C. Yang, K.-W. Chin, Y. Liu, J. Zhang, and T. He, "Robust targets coverage for energy harvesting wireless sensor networks," *IEEE Trans. Veh. Technol.*, vol. 68, no. 6, pp. 5884–5892, Jun. 2019.

[12] B. Gaudette, V. Hanumaiah, M. Krunz, and S. Vrudhula, "Maximizing quality of coverage under connectivity constraints in solar-powered active wireless sensor networks," *ACM Trans. Sensor Netw.*, vol. 10, no. 4, pp. 1–27, Jun. 2014.

[13] C. Yang and K.-W. Chin, "Novel algorithms for complete targets coverage in energy harvesting wireless sensor networks," *IEEE Commun. Lett.*, vol. 18, no. 1, pp. 118–121, Jan. 2014.

[14] X. Ren, W. Liang, and W. Xu, "Quality-aware target coverage in energy harvesting sensor networks," *IEEE Trans. Emerg. Topics Comput.*, vol. 3, no. 1, pp. 8–21, Mar. 2015.

[15] S. Tang, X.-Y. Li, X. Shen, J. Zhang, G. Dai, and S. K. Das, "Cool: On coverage with solar-powered sensors," in *Proc. 31st Int. Conf. Distrib. Comput. Syst.*, Jun. 2011, pp. 488–496.

[16] W.-K. Lee, M. J. W. Schubert, B.-Y. Ooi, and S. J.-Q. Ho, "Multi-source energy harvesting and storage for floating wireless sensor network nodes with long range communication capability," *IEEE Trans. Ind. Appl.*, vol. 54, no. 3, pp. 2606–2615, May 2018.

[17] A. Hossain, P. K. Biswas, and S. Chakrabarti, "Sensing models and its impact on network coverage in wireless sensor network," in *Proc. IEEE Region 10 3rd Int. Conf. Ind. Inf. Syst.*, Kharagpur, India, Dec. 2008, pp. 1–5.

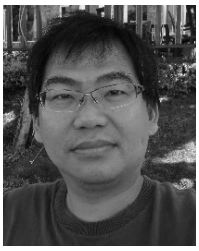

WEN-HWA LIAO (Member, IEEE) received the Ph.D. degree in computer science and information engineering from National Central University, Taiwan, in 2002. He is currently a Full Professor with the Department of Information Management, Tatung University, Taiwan. His current research interests include the Internet of Things, wireless sensor networks, and artificial intelligence. He has served as an Associate Editor for the *International Journal of Distributed Sensor Networks* (IJDSN) and the *International Journal of Vehicle Information and Communication Systems* (IJVICS). He has also served as an Associate Guest Editor for SCI-indexed journal *International Journal of Ad Hoc and Ubiquitous Computing* (IJAHUC).

BHARGAVI DANDE received the M.S. degree in computer science and information engineering from Tamkang University, Taipei, Taiwan, in 2019, where she is currently pursuing the Ph.D. degree in computer science and information engineering. Her current research interests include the Internet of Things, wireless sensor networks, and artificial intelligence.

CHIH-YUNG CHANG (Member, IEEE) received the Ph.D. degree in computer science and information engineering from National Central University, Taiwan, in 1995. He is currently a Full Professor with the Department of Computer Science and Information Engineering, Tamkang University, New Taipei City, Taiwan. His current research interests include the Internet of Things, wireless sensor networks, artificial intelligence, and deep learning. He has served as an Associate Guest Editor for several SCI-indexed journals, including the *International Journal of Ad Hoc and Ubiquitous Computing* (IJAHUC), from 2011 to 2019, the *International Journal of Distributed Sensor Networks* (IJDSN), from 2012 to 2014, *IET Communications*, in 2011, *Telecommunication Systems* (TS), in 2010, the *Journal of Information Science and Engineering* (JISE), in 2008, and the *Journal of Internet Technology* (JIT), from 2004 to 2008.

DIPTENDU SINHA ROY received the Ph.D. degree in engineering from the Birla Institute of Technology, Mesra, India, in 2010. In 2016, he joined the Department of Computer Science and Engineering, National Institute of Technology (NIT) at Meghalaya, India, as an Associate Professor, where he has been serving as the Chair of the Department of Computer Science and Engineering, since January 2017. Prior to his stint at NIT Meghalaya, he had served the Department of Computer science and Engineering, National Institute of Science and Technology at Brahmapur, Brahmapur, India. His current research interests include software reliability, distributed and cloud computing, and the Internet of Things (IoT), specifically applications of artificial intelligence/machine learning for smart integrated systems. He is a member of the IEEE Computer Society.